LETTERS
PUBLISHED ONLINE: 17 JANUARY 2010 | DOI: 10.1038/NNANO.2009.474

nature nanotechnology

Towards a quantum resistance standard based on epitaxial graphene

Alexander Tzalenchuk[1]*, Samuel Lara-Avila[2], Alexei Kalaboukhov[2], Sara Paolillo[3], Mikael Syväjärvi[4], Rositza Yakimova[4], Olga Kazakova[1], T. J. B. M. Janssen[1], Vladimir Fal'ko[5] and Sergey Kubatkin[2]

The quantum Hall effect[1] allows the international standard for resistance to be defined in terms of the electron charge and Planck's constant alone. The effect comprises the quantization of the Hall resistance in two-dimensional electron systems in rational fractions of $R_K = h/e^2 = 25\,812.807\,557(18)\ \Omega$, the resistance quantum[2]. Despite 30 years of research into the quantum Hall effect, the level of precision necessary for metrology—a few parts per billion—has been achieved only in silicon and III–V heterostructure devices[3–5]. Graphene should, in principle, be an ideal material for a quantum resistance standard[6], because it is inherently two-dimensional and its discrete electron energy levels in a magnetic field (the Landau levels[7]) are widely spaced. However, the precisions demonstrated so far have been lower than one part per million[8]. Here, we report a quantum Hall resistance quantization accuracy of three parts per billion in monolayer epitaxial graphene at 300 mK, four orders of magnitude better than previously reported. Moreover, by demonstrating the structural integrity and uniformity of graphene over hundreds of micrometres, as well as reproducible mobility and carrier concentrations across a half-centimetre wafer, these results boost the prospects of using epitaxial graphene in applications beyond quantum metrology.

Graphene—a single layer of graphite—is a truly two-dimensional gapless semiconductor, with electrons mimicking the behaviour of relativistic (Dirac) electrons[9]. This last feature of charge carriers in graphene is manifested most spectacularly through an unusual sequence of the quantum Hall effect (QHE) plateaux[10]. The QHE is a result of the Landau level quantization of the energy spectrum of two-dimensional electrons. In the quantum Hall regime the current is carried by a quantum state, spreading through the whole sample, and the sequence of plateaux in the transverse resistance R_{xy} is determined by the topological (Berry) phase acquired by the charge moving in the magnetic field. This phase is zero in conventional materials, where $R_{xy} = \pm h/ne^2$ (n-integer ≥ 1); it is equal to 2π in bilayer graphene[11,12], leading to a sequence of QHE plateaux at $R_{xy} = \pm(h/4e^2)/(n+1)$ ($n \geq 0$), and it is π in the monolayers[13], which determines the QHE sequence $R_{xy} = \pm(h/4e^2)/(n+1/2)$ ($n \geq 0$), currently regarded as a smoking gun for the sample to contain monolayer graphene[10]. The spacing between the $n=0$ and $n=1$ Landau levels in graphene, $\Delta E^{01}_{\text{graphene}} \approx \sqrt{(B[\text{T}])} \times 36$ meV is large in comparison with conventional materials such as GaAs. For example, at 15 T, $\Delta E^{01}_{\text{graphene}}/\Delta E_{\text{GaAs}} \approx 5.4$.

In reality, an impressive range of unconventional transport properties of electrons in graphene[14], including QHE, have been seen almost exclusively in flakes mechanically exfoliated from bulk graphite. Quantum Hall plateaux have been observed in such material even at room temperature, albeit with an accuracy of 0.2% (ref. 15), while the highest experimentally achieved accuracy[8] of QHE measurements at 300 mK in exfoliated flakes was 15 parts in a million—still modest by metrological standards.

An alternative approach to producing graphene is to grow it epitaxially on silicon carbide (SiC)[16]. Although angle-resolved photoemission studies of epitaxial graphene[17] have revealed an almost linear dispersion of carriers around the corners of a hexagonal Brillouin zone and scanning tunnelling microscopy (STM) showed the sequence of Landau levels typical for graphene[18], Hall resistance quantization has not been observed in epitaxial graphene, in contrast to the exfoliated material, despite numerous attempts. The difficulty was related to the lack of atomically accurate thickness control during film growth on the C-terminated facet, and also a strong variation of carrier density (doping) across the layers grown on the silicon-terminated facet[19].

Here, we demonstrate the viability of a quantum Hall resistance standard based on large-area epitaxial graphene synthesized on the silicon-terminated face of silicon carbide by observation of Hall resistance quantization accurate to a few parts in a billion at 300 mK and a few tens in a billion at 4.2 K. The samples (Fig. 1) studied in our experiments were produced on the silicon-terminated face of a 4H-SiC(0001) substrate (Cree Inc.) using the protocol described in the Methods. We concentrate on the transport characteristics of the smallest and largest of the fabricated devices identified by circles in Fig. 1c. Figure 2a shows the longitudinal (dissipative) R_{xx} and transverse (Hall) R_{xy} resistance of a 11.6 μm × 2 μm Hall bar at 4.2 K and $-14\ \text{T} < B < 14$ T. The absence of positive classical magnetoresistance at magnetic fields $|B| < 2$ T indicates that carrier density in this material is quite homogeneous over the length of at least several micrometres. However, it was noticed that the magnetoresistance was slightly asymmetric with respect to the reversal of the magnetic field direction, which made it difficult to determine the carrier density using the Hall coefficient (although the symmetry was preserved when the voltage leads were swapped with the current leads as the field was reversed). In intermediate magnetic fields we observe Shubnikov–de Haas (SdH) oscillations (as well as a weak localization peak at $|B| < 0.1$ T characteristic of phase coherence electrons in disordered graphene[20]). The analysis of SdH oscillations enabled us to determine the carrier density in this device $n_s = 6.5 \times 10^{11}\ \text{cm}^{-2}$.

Using the density obtained from the SdH oscillations, we estimate that the magnetic field ($B_\nu = hn_s/e\nu$) needed to reach the exact filling factor $\nu = 2$ in this device is ~13.5 T (unfortunately we had no means of controlling the carrier density in these experiments). Two Hall resistance plateaux are clearly visible in Fig. 2a, at $R^{(0)}_{xy} = R_K/2$ ($n=0$) and $R^{(1)}_{xy} = R_K/6$ ($n=1$), corresponding to the filling

[1]National Physical Laboratory, TW11 0LW Teddington, UK, [2]Department of Microtechnology and Nanoscience, Chalmers University of Technology, S-412 96 Göteborg, Sweden, [3]Department of Physics, Politecnico di Milano, 20133 Milano, Italy, [4]Department of Physics, Chemistry and Biology (IFM), Linköping University, S-581 83 Linköping, Sweden, [5]Physics Department, Lancaster University, Lancaster LA1 4YB, UK. *e-mail: alexander.tzalenchuk@npl.co.uk

© 2010 Macmillan Publishers Limited. All rights reserved.

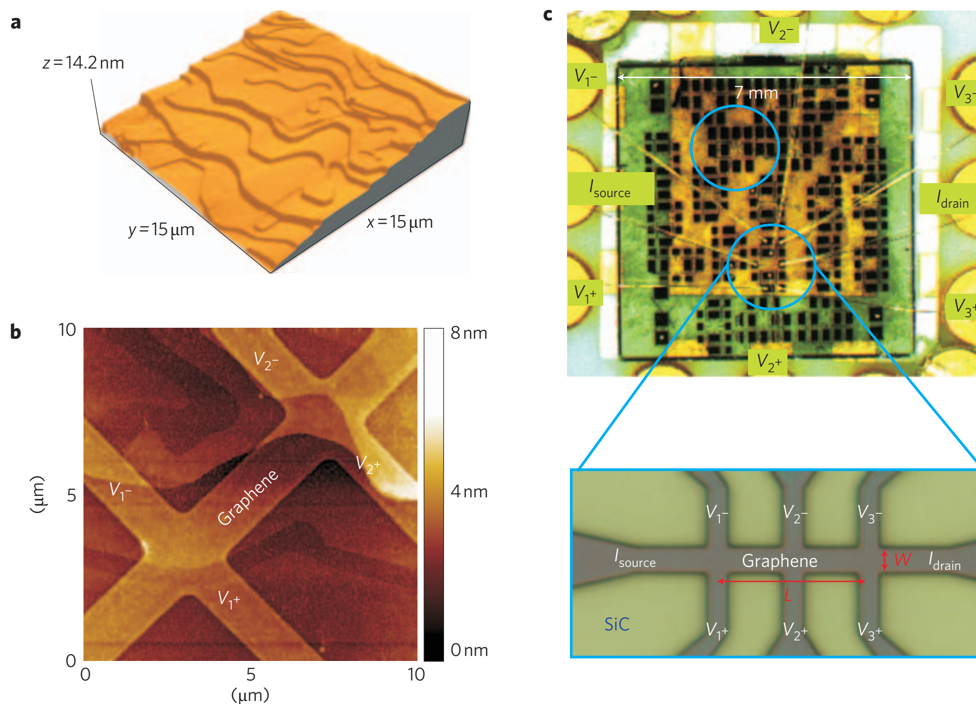

Figure 1 | Sample morphology and layout. **a**, AFM images of the sample: large flat terraces on the surface of the Si-face of a 4H-SiC(0001) substrate with graphene after high-temperature annealing in an argon atmosphere. **b**, Graphene patterned in the nominally 2-µm-wide Hall bar configuration on top of the terraced substrate. **c**, Layout of a 7×7 mm^2 wafer with 20 patterned devices. Encircled are two devices with dimensions $L = 11.6$ µm and $W = 2$ µm (wire bonded) and $L = 160$ µm and $W = 35$ µm, for which the QHE data are presented in Fig. 2. The contact configuration for the smaller device is shown in the enlarged image. To visualize the Hall bar this optical micrograph was taken after oxygen plasma treatment, which formed the graphene pattern, but before the removal of resist.

factors $\nu = 2$ and $\nu = 6$, respectively. In graphene $\nu = 2$ corresponds to the fully occupied zero-energy Landau level characterized by the largest separation $v\sqrt{2\hbar eB/c}$ from other Landau levels in the spectrum, so that the Hall resistance quantization at $R_{xy}^{(0)} = R_K/2$ is particularly robust. This plateau appears already at $|B| \approx 10$ T and is accompanied by a vanishing R_{xx}. The $n = 1$ plateau at $\nu = 6$ is not so flat, with only a weak minimum in R_{xx}, and there is also a visible trace of a structure corresponding to $\nu = 10$. Their presence confirms that the studied material is indeed monolayer graphene.

The magneto-transport measurements on a much bigger, 160 µm × 35 µm Hall bar device (Fig. 1c) are presented in Fig. 2b. A substantial positive magnetoresistance at low fields, which was absent in the smaller sample, indicates that the carrier concentration varies along the larger sample. Because of this, the $\nu = 6$ feature in R_{xx} in the bigger sample is less prominent. Nevertheless, despite the inhomogeneity of the carrier density, the Hall resistance plateau at $R_{xy}^{(0)} = R_K/2$ $(n = 0)$ is robust and is accompanied by vanishing longitudinal resistance R_{xx}. Importantly, the large-area device has a low resistance $R_c \approx 1.5\ \Omega$ of contacts to the graphene layer (determined at the plateau, Fig. 2c) and, when compared to smaller devices, can sustain a much higher current before QHE breaks down, as shown in the $I(V)$ characteristics in Fig. 2d. Because larger breakdown current affords higher-precision measurements in the QHE regime, we chose to perform such measurements in the larger sample. The choice of the field, 14 T, where the most accurate measurements were performed, was determined simply by the limitation of our superconducting magnet. This limit is below $B = 17.5$ T, where the filling factor would be exactly $\nu = 2$ for this sample (with $n_s = 8.5 \times 10^{11}$ cm^{-2} calculated from SdH oscillations).

Precision measurements of R_{xy} were performed in the conditions where R_{xx} is very accurately zero: at $B = 14$ T, $I_{sd} = 2.3$ µA for 4.2 K and $I_{sd} = 11.6$ µA for 300 mK (see Supplementary Information). Note that a higher probe current enables a higher precision of R_{xy} measurements to be achieved, so we performed these studies at 300 mK. The accuracy of Hall resistance quantization in graphene was established in measurements traceable to the GaAs quantum Hall resistance standard using a cryogenic current comparator bridge[21]. Figure 3a shows how the mean relative deviation of $R_{xy}^{(0)}$ from $R_K/2$ depends on the measurement current through the graphene device. The quantization accuracy $+0.4 \pm 3$ parts in 10^9 (mean relative deviation of 129 measurements ± standard error of the mean) inferred from our measurements at 11.6 µA and 300 mK is a four orders of magnitude improvement on the previous best result in exfoliated graphene. This readily puts epitaxial graphene devices in the same league as their semiconductor counterparts. Note that our result was obtained on a sample that is substantially smaller than the semiconductor devices used for calibration and without any optimization. From Fig. 3a it can be seen that graphene is still accurately quantized at 4.2 K; however, at this temperature, the measurement current has to be reduced to 2.3 µA, which increases the uncertainty of the data accumulated over a comparable time interval.

To demonstrate convergence of the measurement process and to see what kind of noise limits the precision of our measurements, in Fig. 3b we plot the Allan deviation[22] of $R_{xy}^{(0)}$ from $R_K/2$ against the measurement time τ. These data follow a $1/\tau^{1/2}$ dependence—behaviour typical of the predominantly white (uncorrelated random) noise. This justifies the use of the standard measures of uncertainty and suggests that these (already very accurate) results can be further improved if one is prepared to measure for longer and at several smaller values of the filling factor within the $R_{xy} = R_K/2$ plateau. Further development should include methods to control the carrier density either chemically or by electrostatic

© 2010 Macmillan Publishers Limited. All rights reserved.

 DOI: 10.1038/NNANO.2009.474

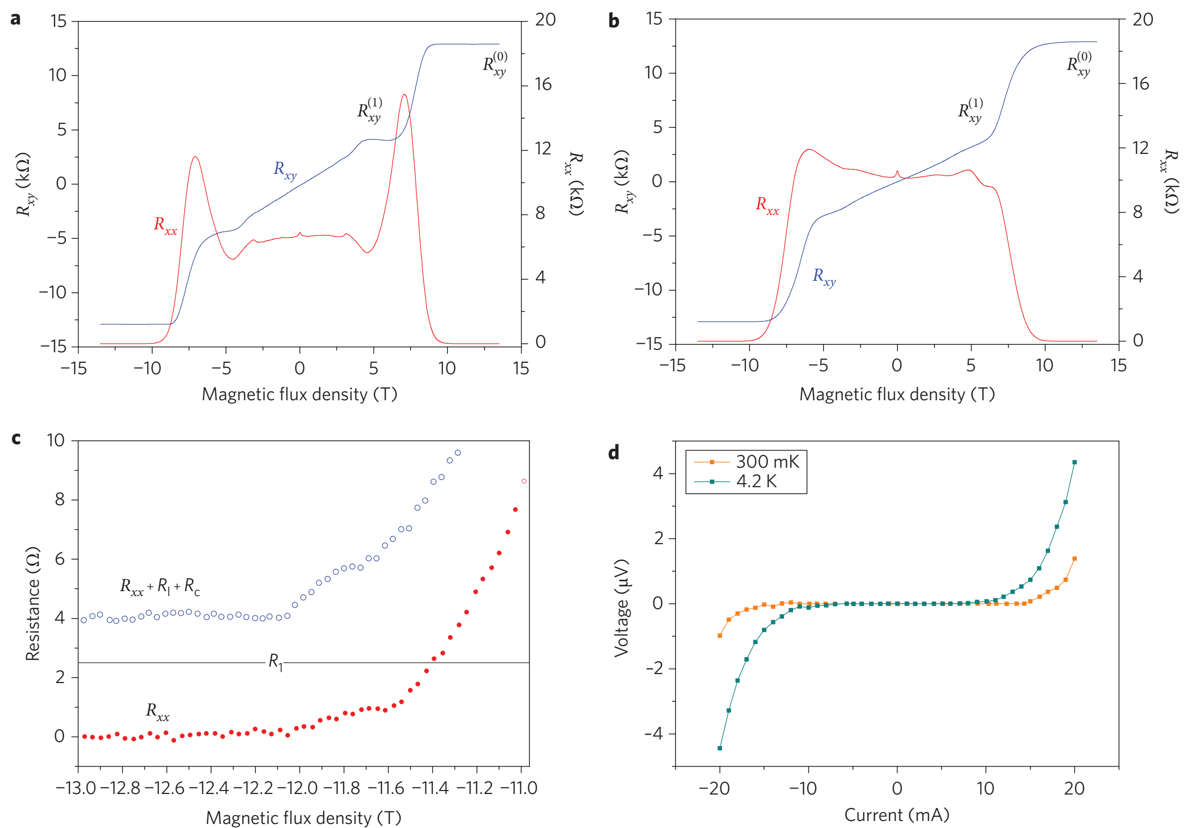

Figure 2 | Quantum Hall effect in epitaxial graphene. a, Transverse (R_{xy}) and longitudinal (R_{xx}) resistance of the 11.6 μm × 2 μm device measured at $T = 4.2$ K with 1 μA current. $R_{xy}^{(0)}$ and $R_{xy}^{(1)}$ represent Hall resistance plateaux at filling factors $\nu = 2$ and $\nu = 6$ respectively. The carrier density $n_s = 6.5 \times 10^{11}$ cm^{-2} was obtained from SdH oscillations. **b**, Transverse (R_{xy}) and longitudinal (R_{xx}) resistance of the 160 μm × 35 μm device measured at $T = 4.2$ K with 1 μA current. The carrier density $n_s = 8.5 \times 10^{11}$ cm^{-2} was obtained from SdH oscillations. **c**, Measurements of the longitudinal resistance R_{xx} performed in a four-point configuration (filled red circles), which excludes contact resistances, and in a three-point configuration (open blue circles), which, as well as R_{xx}, includes the contact resistance R_c and the resistance of the leads from room-temperature electronics down to the sample $R_l = 2.5$ Ω. On the plateau, R_{xx} is very nearly zero and R_c is ∼1.5 Ω for all measured contacts. These measurements were performed while sweeping the magnetic field; hence there is a relatively large spread. **d**, Determination of the breakdown current I_{max} of non-dissipative transport from measurement of the current-voltage characteristic in the longitudinal direction at 14 T: $I_{max} \approx 13$ μA at 300 mK and $I_{max} \approx 5$ μA at 4.2 K. The residual longitudinal resistance was confirmed as $R_{xx} < 0.2$ mΩ at 300 mK measured with $I_{sd} = 12$ μA, and $R_{xx} < 2.4$ mΩ at 4.2 K measured with $I_{sd} = 2.5$ μA.

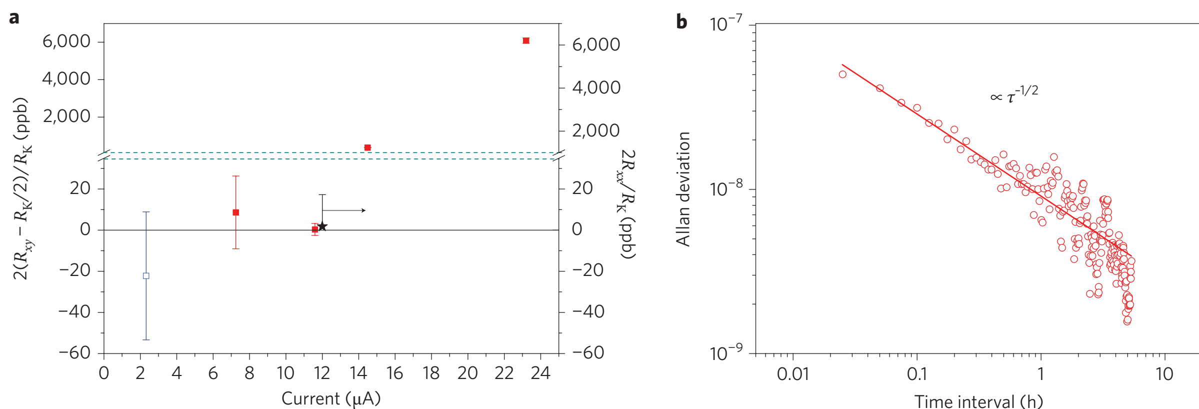

Figure 3 | Determination of Hall resistance quantization accuracy. a, Mean relative deviation of $R_{xy}^{(0)}$ from $R_K/2$ at different bias currents (ppb, parts per billion). The value at the smallest current was measured at 4.2 K (open blue squares), and all other values at 300 mK (filled red squares). The most accurate measurement with an 11.6 μA source-drain current at 14 T and 300 mK was performed over ∼11 h. The value of R_{xx}/R_K determined in the same conditions is also shown (black star) together with the measurement uncertainty. **b**, Allan deviation of $R_{xy}^{(0)}$ from $R_K/2$ versus measurement time τ. The square root dependence indicates purely white noise.

gating, although we believe that the fastest route towards the implementation of graphene in quantum metrology lies in increasing the breakdown current by taking advantage of the flexibility of device design offered by the large area of graphene on a SiC wafer: the optimization of contacts geometry and use of multiple parallel Hall bar devices.

© 2010 Macmillan Publishers Limited. All rights reserved.

To summarize, we report quantum Hall resistance quantization accurate to a few parts in a billion at 300 mK in a large-area epitaxial graphene sample. Several more devices have been studied at 4.2 K, demonstrating quantization within an accuracy of some tens in 10^9, confirming the robustness of the QHE in graphene synthesized on the silicon-terminated face of SiC. This remarkable precision constitutes an improvement of four orders of magnitude over the best previous results obtained in exfoliated graphene, and is similar to the accuracy achieved in the established semiconductor resistance standards. In the future, improvements in measurement precision may advance the understanding of the QHE effect itself, by determining whether there exist systematic deviations of the quantized Hall resistance in graphene from the fundamental values at the rational fractions of h/e^2. Even more importantly, the experiments have demonstrated structural integrity over hundreds of micrometres and revealed relative uniformity of epitaxial graphene across a half-centimetre SiC wafer (as well as from wafer to wafer). This supports the potential of SiC technology for microelectronics applications possibly extending far beyond quantum metrology.

Methods

The material used in the reported experiments was produced on the Si-face of SiC; the reaction kinetics is slower there than on the C-face because of the higher surface energy. This aids in the well-controlled formation of homogeneous graphene[23]. Graphene was grown at 2,000 °C and 1 atm argon gas pressure, resulting in monolayers of graphene atomically uniform over more than 50 μm^2, as confirmed by low-energy electron microscopy. Twenty Hall bar devices of different sizes, from 160 $\mu m \times 35$ μm down to 11.6 $\mu m \times 2$ μm were produced on two 0.5-cm^2 wafers using standard electron-beam lithography and oxygen plasma etching (Fig. 1c). Atomic force microscopy (AFM) images reveal that the graphene layer covers the substrate steps like a carpet, preserving its structural integrity (Fig. 1a). Contacts to graphene were produced by straightforward deposition of 3 nm of titanium and 100 nm of gold through a lithographically defined mask followed by lift-off, with a typical area of graphene–metal interface of 1×10^4 μm^2 for each contact. This process favourably compares with the laborious contact preparation to two-dimensional electron gas in conventional semiconductor technology. The manufactured devices were not cleaned in any way before measurements. Using low-magnetic-field measurements, we established that the manufactured material was *n*-doped, owing to charge transfer from SiC, with the measured electron concentration lying in the range 5×10^{11} to 10×10^{11} cm^{-2}, mobility of $\sim$2,400 $cm^2\,V^{-1}\,s^{-1}$ at room temperature and between 4,000 and 7,500 $cm^2\,V^{-1}\,s^{-1}$ at 4.2 K, almost independent of device dimensions and orientation with respect to the substrate terraces. The scattering mechanisms in the epitaxial graphene and the role of the substrate need further investigation. As seen in the AFM images (Fig. 1b), the graphene Hall bars are patterned across many substrate terraces; however, the measurements of the QHE reveal that the continuity of graphene is preserved.

Received 14 September 2009; accepted 3 December 2009; published online 17 January 2010; corrected online 23 February 2010

References

1. von Klitzing, K., Dorda, G. & Pepper, M. New method for high-accuracy determination of the fine-structure constant based on quantized Hall resistance. *Phys. Rev. Lett.* **45,** 494–497 (1980).
2. Mohr, P. J., Taylor, B. N. & Newell, D. B. CODATA recommended values of the fundamental physical constants: 2006. *Rev. Mod. Phys.* **80,** 633–730 (2008).
3. Jeckelmann, B. & Jeanneret, B. The quantum Hall effect as an electrical resistance standard. *Rep. Progr. Phys.* **64,** 1603–1655 (2001).
4. Delahaye, F. *et al.* Precise quantized Hall resistance measurements in $GaAs/Al_xGa_{1-x}As$ and $In_xGa_{1-x}As/InP$ heterostructures. *Metrologia* **22,** 103–110 (1986).
5. Piquemal, F. *et al.* Report on a joint BIPM-EUROMET project for the fabrication of QHE samples by the LEP. *IEEE Trans. Instrum.* **42,** 264–268 (1993).
6. Poirier, W. & Schopfer, F. Resistance metrology based on the quantum Hall effect. *Eur. Phys. J. Spec. Top.* **172,** 207–245 (2009).
7. Landau, L. D. Diamagnetismus der Metalle. *Z. Phys.* **64,** 629–637 (1930).
8. Giesbers, A. J. M. *et al.* Quantum resistance metrology in graphene. *Appl. Phys. Lett.* **93,** 222109 (2008).
9. Novoselov, K. S. *et al.* Two-dimensional gas of massless Dirac fermions in graphene. *Nature* **438,** 197–200 (2005).
10. Zhang, Y. B. *et al.* Experimental observation of the quantum Hall effect and Berry's phase in graphene. *Nature* **438,** 201–204 (2005).
11. Novoselov, K. S. *et al.* Unconventional quantum Hall effect and Berry's phase of 2π in bilayer graphene. *Nature Phys.* **2,** 177–180 (2006).
12. McCann, E. & Fal'ko, V. I. Landau-level degeneracy and quantum Hall effect in a graphite bilayer. *Phys. Rev. Lett.* **96,** 086805 (2006).
13. Neto, A. H. C. *et al.* The electronic properties of graphene. *Rev. Mod. Phys.* **81,** 109–162 (2009).
14. Geim, A. K. Graphene: status and prospects. *Science* **324,** 1530–1534 (2009).
15. Novoselov, K. S. *et al.* Room-temperature quantum Hall effect in graphene. *Science* **315,** 1379–1379 (2007).
16. Virojanadara, C. *et al.* Homogeneous large-area graphene layer growth on 6H-SiC(0001). *Phys. Rev. B* **78,** 245403 (2008).
17. Bostwick, A. *et al.* Quasiparticle dynamics in graphene. *Nature Phys.* **3,** 36–40 (2007).
18. Miller, D. L. *et al.* Observing the quantization of zero mass carriers in graphene. *Science* **324,** 924–927 (2009).
19. Darancet, P. *et al.* Quenching of the quantum Hall effect in multilayered epitaxial graphene: the role of undoped planes. *Phys. Rev. Lett.* **101,** 116806 (2008).
20. McCann, E. *et al.* Weak-localization magnetoresistance and valley symmetry in graphene. *Phys. Rev. Lett.* **97,** 146805 (2006).
21. Kleinschmidt, P., Williams, J. M., Fletcher, N. E. & Janssen, T. Cryogenic current comparator bridge for quantum Hall resistance ratio measurements. *IEE Proc. Sci. Meas. Technol.* **149,** 302–304 (2002).
22. Allan, D. W. Should the classical variance be used as a basic measure in standards metrology? *IEEE Trans. Instrum. Meas.* **36,** 646–654 (1987).
23. Emtsev, K. V. *et al.* Towards wafer-size graphene layers by atmospheric pressure graphitization of silicon carbide. *Nature Mater.* **8,** 203–207 (2009).

Acknowledgements

The authors would like to thank L. Walldén, T. Löfwander, F. Lombardi, J. Gallop and T. Claeson for stimulating discussions and S. Giblin and J. Williams for help with experiments. We are grateful to the NPL Strategic research programme, Swedish Research Council and Foundation for Strategic Research, European Union FP7 SINGLE, UK Engineering and Physical Sciences Research Council grant no. EP/G041954 and the Science & Innovation Award EP/G014787 for financial support.

Author contributions

S.K., A.T. and V.F. conceived and designed the experiments. A.T., S.L., A.K., S.P., O.K., T.J. and S.K. performed the experiments. R.Y. and M.S. contributed materials. A.T., V.F. and S.K. analysed the data and co-wrote the paper. All authors discussed the results and commented on the manuscript.

Additional information

The authors declare no competing financial interests. Supplementary information accompanies this paper at www.nature.com/naturenanotechnology. Reprints and permission information is available online at http://npg.nature.com/reprintsandpermissions/. Correspondence and requests for materials should be addressed to A.T.

© 2010 Macmillan Publishers Limited. All rights reserved.